Cancer Cell
Article

Transient Inhibition of the Hedgehog Pathway in Young Mice Causes Permanent Defects in Bone Structure

Hiromichi Kimura,[1,3] Jessica M.Y. Ng,[2] and Tom Curran[2,*]
[1]Department of Developmental Neurobiology, St. Jude Children's Research Hospital, 332 North Lauderdale Street, Memphis, TN 38105, USA
[2]Department of Pathology and Laboratory Medicine, The Joseph Stokes Jr. Research Institute, The Children's Hospital of Philadelphia, 517 Abramson Research Center, 3615 Civic Center Boulevard, Philadelphia, PA 19104, USA
[3]Present address: Pharmaceutical Research Division, Pharmacology Research Laboratories II, Takeda Pharmaceutical Company Ltd., 10 Wadai, Tsukuba, Ibaraki, 300-4293, Japan.
*Correspondence: currant@chop.edu
DOI 10.1016/j.ccr.2008.01.027

SUMMARY

The Hedgehog (Hh) pathway plays critical roles in normal development and in tumorigenesis. We generated Gli-luciferase transgenic mice to evaluate the Smo inhibitor, HhAntag, by whole animal functional imaging. HhAntag rapidly reduced systemic luciferase activity in 10- to 14-day-old mice following oral dosing. Although pathway activity was restored 2 days after drug removal, brief inhibition caused permanent defects in bone growth. HhAntag inhibited proliferation and promoted differentiation of chondrocytes, leading to dramatic expansion of the hypertrophic zone. After drug removal, osteoblasts invaded the cartilage plate, mineralization occurred, and there was premature fusion of the growth plate resulting in permanent disruption of bone epiphyses.

INTRODUCTION

Signal transduction pathways govern cell proliferation and differentiation throughout development. Persistent signaling, as a consequence of mutation or epigenetic modulation of specific pathway components in cancer cells, promotes unrestrained cell growth and can result in tumorigenesis. Recent studies support the notion that targeting aberrantly activated signal transduction pathways in selected cancers, using small molecule inhibitors, greatly increases response rates while reducing toxic side effects (Arora and Scholar, 2005; Savage and Antman, 2002; Silvestri and Rivera, 2005). The hedgehog (Hh) pathway provides an attractive potential target in many cancers because of its proposed widespread role in maintaining cancer stem cells, either intrinsically or extrinsically (Dellovade et al., 2006). Hh signaling is critical for many processes during embryonic and postnatal development, including proliferation, differentiation, cell fate specification, left-right asymmetry, and morphogenesis (McMahon et al., 2003). Sporadic and familial mutations in the Hh pathway genes, *patched-1* (*PTCH1*), *suppressor-of-fused* (*SUFU*), and *smoothened* (*SMO*), leading to elevated expression of downstream target genes including *GLI1*, have been reported in basal cell carcinoma (BCC) and the pediatric brain tumor medulloblastoma (MB) (Fogarty et al., 2005; Gorlin, 1995). In addition, growth of many cancers has been suggested to depend on continuous Hh signaling even in the absence of activating mutations in the pathway (Evangelista et al., 2006).

Potential therapeutic agents specific for the Hh pathway were identified initially as plant alkaloid teratogens that cause holoprosencephaly when ingested by pregnant sheep during a critical period in the first trimester (Binns et al., 1963; Binns et al., 1965; Keeler, 1972). Subsequently, they were shown to function by binding to SMO to block downstream signaling, thus inhibiting proliferation (Chen et al., 2002; Cooper et al., 1998). Several structurally unrelated compounds have now been isolated that function in the same manner (Gabay et al., 2003; Williams

SIGNIFICANCE

Hh pathway inhibitors are currently being developed as potential therapies for several cancers, including pediatric medulloblastoma. Functional imaging studies in young mice demonstrated that blocking the pathway for as little as 2 days caused permanent defects in bone growth. The aberrant structures formed could not be removed by bone remodeling, so the defects were permanent. These results demonstrate a requirement for uninterrupted Hh pathway signaling during postnatal bone development. In addition, our findings raise concerns about the use of Hh pathway inhibitors in pediatric patients, and they point to a broader issue regarding the use of signal transduction inhibitors in children.

et al., 2003). These agents have attracted a great deal of attention as potential anticancer therapies, particularly in tumors carrying *PTCH1* mutations such as BCC and MB (Athar et al., 2004; Berman et al., 2002; Romer et al., 2004; Sanchez and Ruiz i Altaba, 2005). In mice, heterozygous mutation of *Patched-1* (*Ptc1*) results in a 20% incidence of MB, and this is accelerated to 100% on a p53 null background (Goodrich et al., 1997; Kimura et al., 2005; Wetmore et al., 2000; Wetmore et al., 2001). Previously, we conducted proof-of-principle studies in these mice using an inhibitor of SMO (HhAntag) (Romer et al., 2004). Treatment of mice with HhAntag eradicated spontaneous MB without causing any serious side effects. The findings were confirmed in transplantation models, using tumors from a variety of mouse MBs, including some with no known mutations in the Hh pathway (Sasai et al., 2006, 2007). These results encouraged us to consider the use of Smo inhibitors for treatment of the subset of childhood MB in which the Shh pathway is activated (Thompson et al., 2006).

As a next step in this process, we developed a functional imaging system for the analysis of Hh pathway antagonists in vivo. Here, we show that GliLuc mice can be used to monitor the response of the Shh pathway to agonists and antagonists by intravital imaging. Treatment of young mice with as little as two doses of 100 mg/kg HhAntag within a 24 hr period transiently inhibited Hh pathway activity, which was restored 48 hr after drug removal. However, to our surprise, brief exposure to the Smo inhibitor resulted in permanent defects in bone development. HhAntag blocked proliferation of chondrocytes promoting differentiation and expansion of the hypertrophic zone. Shortly after drug removal, there was a dramatic increase in mineralization leading to premature fusion of the growth plate and inappropriate synthesis of trabecular bone. The disruption of the bone epiphyses persisted in adults resulting in shortening of the bones and aberrant joint structures. Even transient exposure to HhAntag resulted in a dramatic loss of proliferating chondrocytes, depletion of the progenitor pool, and permanent disruption of the growth plate. These findings raise serious concerns about the use of Hh pathway antagonists in children and they pose a broader question about the potential developmental toxicities of signal transduction inhibitors. Since many signaling pathways fulfill specific roles during development, it would be prudent to investigate the effects of molecular targeted therapies in developing animal models prior to their use in pediatric patients.

RESULTS

Generation of GliLuc Mice and Functional Imaging of Hh Pathway Activity

Hh activity can be readily monitored by optical imaging in cells transfected with a plasmid containing eight Gli binding sites fused to the δ-crystallin basal promoter and the firefly luciferase gene (Kamachi and Kondoh, 1993; Sasaki et al., 1997). We used this same construct to generate six independent lines of transgenic mice by microinjection. Primary granule cell cultures were prepared from litters obtained from each strain and tested for their ability to respond to Shh. Five lines did not show any change in luciferase activity in response to Shh, perhaps because transgene expression was suppressed by sequences surrounding the site of integration. However, one line exhibited a robust Shh-induced increase in luciferase activity and this was selected to generate a cohort of GliLuc mice for future studies.

The Hh pathway is very active during embryogenesis and postnatal central nervous system development (McMahon et al., 2003). As expected, GliLuc transgenic embryos (visualized through the skin of the dam) exhibited a robust luciferase signal within 15 min of inoculating the dam with 150 mg/kg D-Luciferin by intraperitoneal (IP) injection (Figure 1A). As gestation progressed, GliLuc transgenic embryos showed increased luciferase activity (Figure 1A). Embryos isolated at E17.5 were positive, with a particularly strong signal emanating from the developing brain (Figure 1B).

To determine the ability of the transgene to respond to Shh stimulation, mouse embryo fibroblast (MEF) cultures were prepared and treated with Shh for 48 hr before measuring the level of luciferase activity. As shown in Figure 1C, as little as 50 ng/ml Shh caused a dramatic increase in luciferase activity when measured by bioluminescence imaging or chemiluminescence biochemical assays. The maximal response was obtained with 100 ng/ml Shh, which is identical to the concentration required to promote maximal proliferation of primary granule cells in culture (data not shown). Since there was no basal activity in untreated fibroblasts, it is not meaningful to calculate a fold response. The ability of HhAntag to block Hh signaling was determined using a dose of 100 ng/ml Shh. The half-maximal response (EC_{50}) was observed at a concentration of 0.15 μM HhAntag. This is consistent with previous reports using transfected cell lines (Romer et al., 2004).

The ability of HhAntag to suppress Hh pathway activity in embryos was investigated by treating pregnant dams with HhAntag at 100 mg/kg twice daily by oral gavage at both E13.5 and E14.5 (Figure 1A). The signals observed from treated embryos were diminished compared to those from untreated embryos. At the end of the study we examined the embryos and found evidence of shortened limbs as a consequence of exposure to HhAntag (data not shown).

To examine Hh pathway activity during postnatal development, we quantified the GliLuc signal in pups from postnatal days 1, 7, and 14, as well as in young adults at 5 and 11 weeks of age (Figure 1D). Hh pathway activity was very high shortly after birth, and then it progressively declined throughout the course of postnatal development (Figure 1D). Little or no GliLuc signal was detected in 11-week-old mice. Although the imaging approach mostly detects superficial signals in skin tissue, the skin still exhibited the highest level of pathway activity when compared with other dissected mouse tissues including brain, liver, lung, kidney, heart, and spleen (data not shown). During early mouse postnatal development, epidermal and dermal progenitors actively proliferate to form hair and nonhair epithelium as well as stratified epidermis (Fuchs, 2007), and proliferation of these progenitors cells is under tight control by the Hh pathway (Callahan and Oro, 2001). However, in contrast, in the adult skin epithelium, the expression levels of Shh, Gli1, and Gli2 are very low.

Hh Pathway Activity Is Temporarily Inhibited in Young Mice Treated with HhAntag

To evaluate the ability of HhAntag to inhibit Hh pathway activity in vivo, we imaged luciferase activity in young GliLuc mice following treatment with HhAntag (Figure 2). Previously, we found

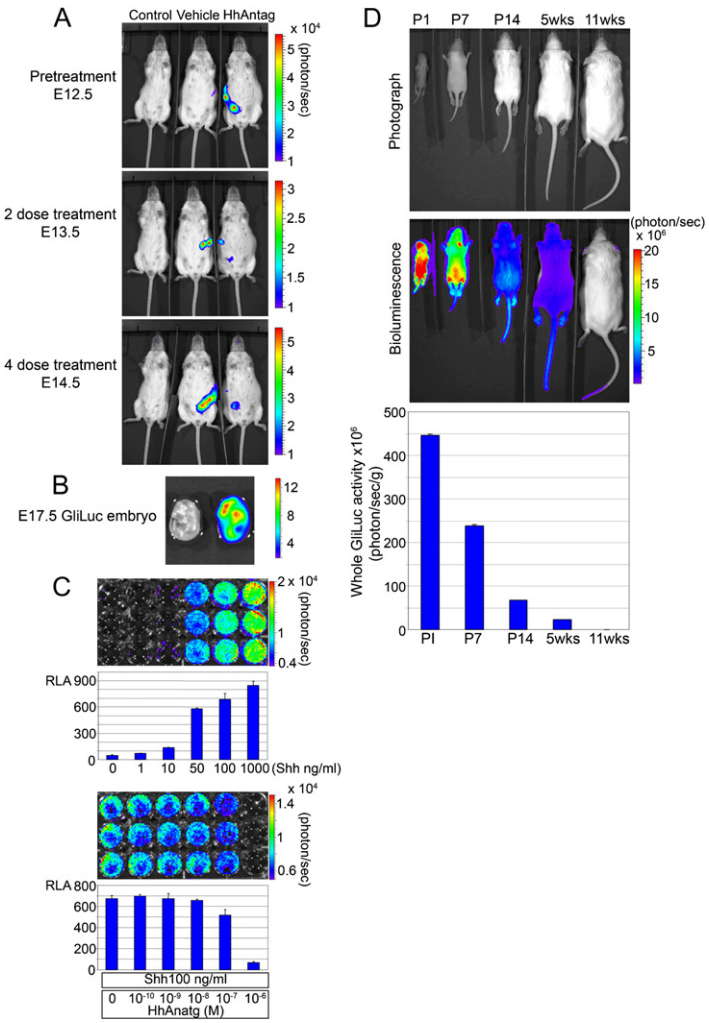

Figure 1. Functional Imaging of Shh Pathway Activity in GliLuc Transgenic Mice

(A) Images of wild-type female mice previously mated with a transgenic GliLuc male mouse after injection of 150 mg/kg D-Luciferin. Control and pregnant (Vehicle- and HhAntag-treated) mice were placed on their backs and imaged using a Xenogen IVIS200 Bioimaging system. Pregnant mice were imaged at 12.5 days postcoitum (dpc) (pretreatment), at 13.5 dpc (two-dose treatment), and 14.5 dpc (four-dose treatment). Mice were imaged untreated (control), 5 hr after treatment with Vehicle, or with 100 mg/kg HhAntag.

(B) Images of wild-type and GliLuc transgenic embryos at 17.5 dpc. Embryos were removed after intraperitoneal inoculation of the dam with D-Luciferin.

(C) Cell-based bioluminescence images (upper) and luminescence assays (lower) of MEFs from GliLuc mice at E13.5 treated with increasing doses of Shh. RLA, relative luciferase activity. Data are the mean ± SD (triplicate).

(D) Downregulation of Hh pathway activity during postnatal development. Grayscale photograph and bioluminescence images of GliLuc mice at P1, P7, and P14 as well as 5 and 11 weeks of age. Graph shows the Gliluc signal intensity (photons per second) per body weight (gram). Data indicate mean ± SD (n = 3).

that treatment of *Ptc1*$^{+/-}$*p53*$^{-/-}$ mice with HhAntag, given twice daily by oral gavage at 100 mg/kg, downregulates Gli1 expression in tumor cells within 4 days and eradicates tumor volume after 2 weeks (Romer et al., 2004; Sasai et al., 2006). Lowering the dose of HhAntag to 20 mg/kg caused partial suppression of Gli1 expression and incomplete regression of MB. Here, GliLuc mice were treated at postnatal day 10 (P10), with a range of HhAntag doses (10, 25, 50, and 100 mg/kg), twice daily by oral gavage, and the level of luciferase activity suppression after 1 and 2 days of treatment was quantified (Figure 2A). The results indicated that HhAntag partially blocked Hh pathway activity in skin at 10 mg/kg and completely suppressed activity at 25, 50, and 100 mg/kg HhAntag (Figure 2B). A strong GliLuc signal was observed in the head of treated mice, perhaps because the thinner skull in young mice is less effective at blocking the luciferase signal from the brain (Figure 2).

The time course of inhibition was monitored in GliLuc mice treated with 100 mg/kg HhAntag twice daily for a total of eight doses from P10 to P14. After two doses, the level of Hh pathway activity was significantly decreased (Figures 2C–2E). The reduction in activity was sustained throughout the entire treatment period (Figure 2F). Two doses of HhAntag were sufficient for maximum suppression of Hh pathway activity as the GliLuc signal was not further reduced by additional treatment. Pathway activity recovered within 2 days of drug removal (Figure 2G). These data demonstrate that suppression of Hh pathway activity by HhAntag in young mice is transient and rapidly reversible.

Previous studies indicated that cyclopamine, a naturally occurring plant alkaloid, caused regression of MB and other tumors in several mouse transplantation models (Berman et al., 2002, 2003; Karhadkar et al., 2004; Sanchez et al., 2005). In vitro, cyclopamine is approximately 10-fold less active than HhAntag at suppressing Hh activity (Romer et al., 2004). We compared the effects of cyclopamine and HhAntag on Hh pathway activity in young GliLuc mice. We were precluded from using cyclopamine at higher doses due to toxic side effects. Therefore, cyclopamine or HhAntag were given orally, twice daily, at 50 mg/kg. Cyclopamine reduced the level of GliLuc activity in treated mice but it was less potent than HhAntag, even after a total of eight doses (see Figures S1A and S1B available online). These in vivo data are comparable with previous studies carried out in cell culture experiments (Romer et al., 2004; Williams et al., 2003) (Figure S1). After drug removal, Hh pathway activity rapidly recovered, as observed previously with HhAntag treatment (Figure S1C and Figure 2G). Longer treatment periods were not possible due to acute weight loss and dehydration in cyclopamine-treated mice (Figure S1D). Thus, because of the dose-limiting toxicity, cyclopamine cannot be used to completely suppress systemic GliLuc activity in vivo.

Transient Exposure of Young Mice to HhAntag Causes Permanent Bone Defects

In our previous studies in adult mice, we did not observe any weight loss or growth retardation following twice daily treatment with 100 mg/kg HhAntag for 2 weeks. Therefore, we were surprised to note that young mice, from P10 to P14, treated with HhAntag did not thrive. In fact, they lost weight during the period of drug treatment (Figure 3A, day 10 to 14). However, the effect of

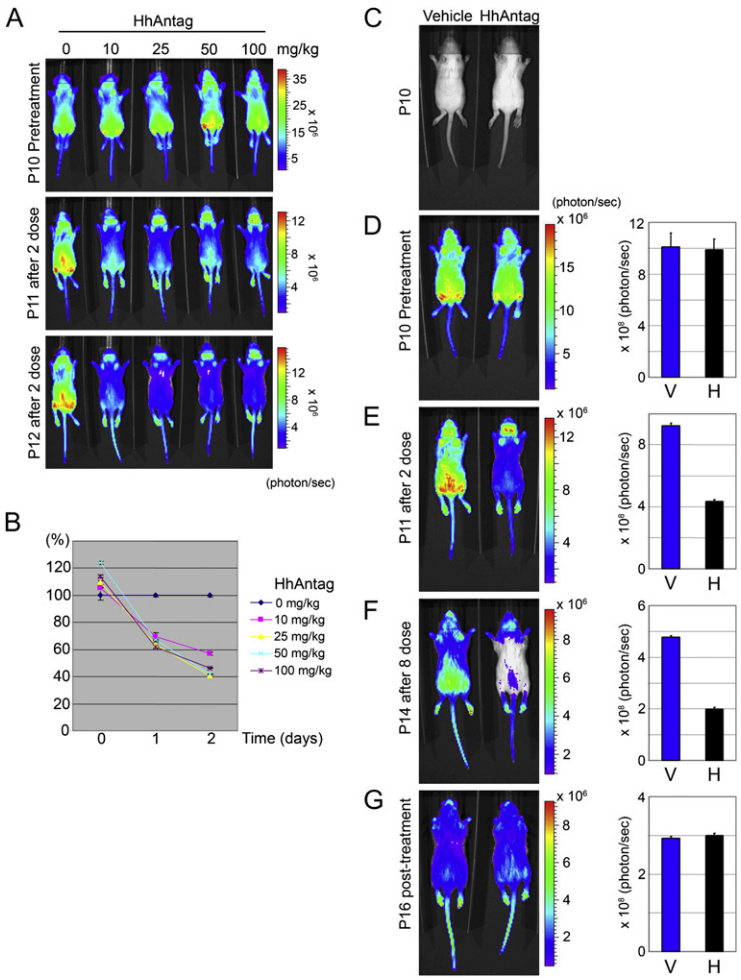

Figure 2. Vital Imaging of Hh Pathway Suppression by HhAntag in Young Mice

(A) Dose-dependent suppression of GliLuc activity by HhAntag. Five GliLuc transgenic males at P10 were treated with HhAntag at the indicated drug concentrations. Bioluminescence images were captured at P11 (1 day after HhAntag treatment) and at P12 (2 days after treatment).

(B) Graph showing quantitation of Hh pathway activity at each dose. Signals were measured on three different images obtained from each mouse after D-Luciferin had equilibrated. Values shown are mean ± SD. Activity in the mouse treated with 0 mg/kg (blue diamonds) was designated as 100%. Pink squares, HhAntag 10 mg/kg; yellow triangles, 25 mg/kg; light blue crosses, 50 mg/kg; purple stars, 100 mg/kg.

(C–G) Time-course of Hh pathway suppression and recovery. Grayscale photographs of P10 mice (given Vehicle or 100 mg/kg HhAntag) were compared with images and graphs of bioluminescence signals in the same two mice at P10 (before treatment), P11 after two doses of HhAntag, P14 after eight doses, and P16 2 days after the eight-dose treatment period. Values shown are mean ± SD. V, Vehicle; H, HhAntag.

HhAntag was less severe than that observed with cyclopamine, and we did not see any evidence of dehydration. Although the HhAntag-treated mice regained weight after cessation of treatment, they never caught up with their littermates (Figure 3A), and they remained noticeably smaller than control mice even long after the brief 4 day treatment period (Figure S2A). This suggested that short-term treatment with HhAntag permanently altered growth.

X-ray analysis revealed widespread abnormalities of the skeleton in GliLuc mice treated with HhAntag (Figure 3B). In all treated mice, we found shortened endochondral bones, and several also displayed grossly abnormal bone structures, particularly the femur and tibia. Whole skeleton staining with Alizarin Red S revealed significant joint abnormalities (Figure 3C) similar to those reported in young mice in which *Ihh* is conditionally mutated at P0 (Maeda et al., 2007). Histological analysis of longitudinal sections of femurs from 12-week-old mice, previously treated with HhAntag between P10–P14, revealed malformation of the epiphysis and growth plate (Figure 3D, upper panels, and Figures S2A and S2C). The columnar organization of chondrocytes in the growth plate was disrupted, and the cartilage structure appeared dysplastic (Figure 3D, lower panels). The extensive defects in bone growth were not accompanied by any other major defects in other organs as determined by gross examination and necropsy of 12-week-old treated mice. These observations are consistent with the critical role the hedgehog pathway is known to play in bone development (Ehlen et al., 2006). Deletion of Indian Hh (Ihh) causes embryonic lethality in mice (St-Jacques et al., 1999), conditional ablation results in a phenotype similar to that reported here (Maeda et al., 2007), and hypomorphic mutations of *IHH* in humans cause acrocapitofemoral dysplasia (Hellemans et al., 2003).

We investigated the effects of HhAntag treatment duration on bone development in normal mice. Mice were treated with 100 mg/kg HhAntag at P10 twice daily for 1–4 days, and the effects on bone development were analyzed at 6 weeks of age. We observed an obvious decrease in the growth of the long bones after only 2–4 days of treatment (equivalent to four to eight doses of HhAntag, Figure 4B). More modest effects were observed on bone morphology in mice receiving only two doses of HhAntag over a 24 hr period (Figure 4B). Histological analysis of long bones from mice receiving six doses of HhAntag indicated malformation of the epiphysis similar to that observed in mice receiving eight doses (Figure 3D and 4E). More subtle defects were observed in the growth plate after four doses of HhAntag (Figure 4D). However, even with as little as two doses of HhAntag, we detected aberrations in the femur growth plate (Figure 4E). Extending the duration of treatment was correlated with progressive shortening of the femur, bowing of the fibula, and joint malformation (Figure 4).

Next, we analyzed the effects of different concentrations of HhAntag on bone development. Persistent bone defects were observed in adult mice after exposure to escalating concentrations of HhAntag, given twice daily over a period of 4 days, between P10 and P14 (Figure S3). No gross malformations were detected at the lowest concentration tested (10 mg/kg), and the normal columnar chondrocytic structure was present (Figures S3B, S3F, and S3J). However, at 25 mg/kg, abnormal bone formation was observed in the femur epiphysis, and the

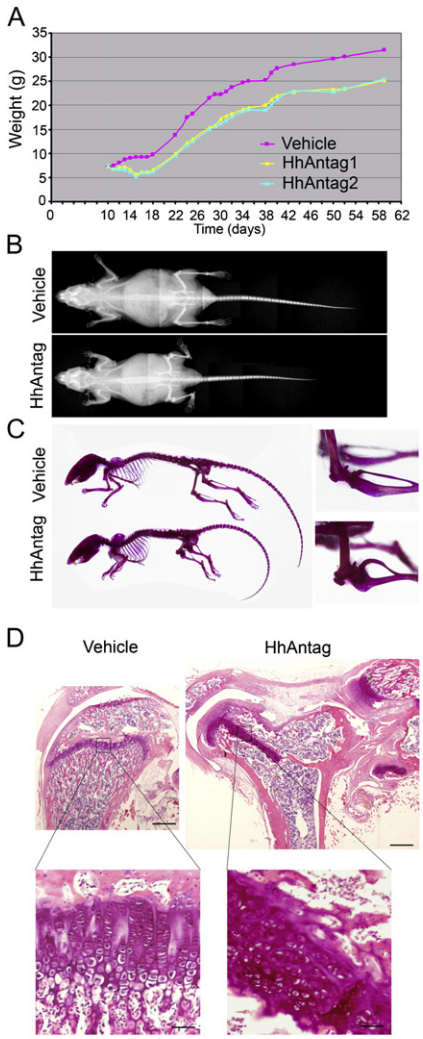

Figure 3. HhAntag Causes Bone Defects

(A) Changes in body weight during and after 100 mg/kg HhAntag treatment (pink, Vehicle; yellow and blue, of two wild-type mice and two HhAntag-treated mice, HhAntag 1 and 2).

(B) Soft X-ray images of 12-week-old mice after eight doses of HhAntag (upper, Vehicle; lower, HhAntag).

(C) Skeletal staining of 12-week-old mice treated with Vehicle or with 100 mg/kg HhAntag between P10 and P14. Insets show magnified knee joints.

(D) H&E staining of longitudinal cross-sections of femurs in 12-week-old mice after eight doses of Vehicle or HhAntag. Magnified regions show details of the growth plate. Bars indicate 250 μm (upper panels) and 50 μm (lower panels).

structures of the growth plate and articular cartilage were altered (Figure S3C). Instead of the expected zones of maturation, hypertrophy, and calcification, there appears to be a residual zone of proliferation surrounded by newly synthesized bone. The femur growth plate seemed more sensitive than that of the tibia as discontinuities appeared at 25 mg/kg in the femur but not in the tibia (Figures S3C, S3G, and S3K). The tibia growth plate was clearly disrupted at a concentration of 100 mg/kg HhAntag (Figures S3D, S3H, and S3L). Thus, dose escalation of HhAntag resulted in progressive disruption of bone development in young mice.

HhAntag Blocks Proliferation and Rapidly Promotes Differentiation of Chondrocytes

Two days of exposure to HhAntag at 100 mg/kg was sufficient to downregulate whole body GliLuc activity (Figure 5A). Although, by gross analysis (Alizarin Red S and Alcian blue staining), the skeleton appeared normal at P12 (Figures S4A–S4E), there was a dramatic expansion of the hypertrophic zone in the growth plate (Figure 5B). Safarin O staining revealed disrupted matrix deposition and premature entry of proliferating chondrocytes into the terminal hypertrophic state, indicating that the growth plate had started to withdraw and the columnar organization of maturing hypertrophic chondrocytes was beginning to break down (Figures S6B and S6D). There was also a reduction and altered morphology of the perichondrial cell population abutting the hypertrophic zone (Figures 5C and 5D). After 4 days of treatment, the bone collar was clearly diminished (Figure 5D, arrowheads). *Ihh* is also known to affect perichondrial cells, including osteoblast progenitors. During embryonic bone development, $Ihh^{-/-}$ embryos display cortical bone defects as well as aberrant chondrocyte development in the long bones (Colnot et al., 2005; St-Jacques et al., 1999).

The expansion of the hypertrophic zone was accompanied by a dramatic decrease in the number of proliferating chondrocytes in the upper layer of the growth plate, as determined by 5-bromo-2-deoxyuridine (BrdU) labeling (Figure 5E). HhAntag also appeared to reduce proliferation of osteoblasts (Figures S5E and S5B). Quantitatively, the number of osteoblasts in the sampled area was reduced by 54.6% ± 16 ($n = 6$, $p = 0.012$) after 2 days of treatment and 49.8% ± 20 ($n = 6$, $p = 0.002$) after 4 days of treatment.

Withdrawal of HhAntag Promotes Osteogenesis and Bone Remodeling

The Hh pathway was rapidly restored after cessation of HhAntag treatment in young mice; however, the defects in bone structure persisted in adults, indicating that bone remodeling was unable to repair the structural defects precipitated by HhAntag. Although there was an increase in bone matrix in the growth plate during the course of treatment, particularly at the chondro-osseus junction, this dropped precipitously 2 days after HhAntag removal (Figure 6A and Figure S6). Two days after cessation of treatment, the integrity of chondrocyte columnar layers was lost, and large, irregular spicules containing many osteocytes appeared in cartilaginous regions (Figure S6F).

Analyses of bone tissue, using markers for several cell populations including osteoblasts (*Col I*), prehypertrophic chondrocytes (*Col II*), and hypertrophic chondrocytes (*Col X*) (Figures 6A–6D), indicated that the chondrocyte population dropped dramatically, and the distribution of osteoblasts changed shortly after HhAntag treatment. It is possible that osteoblasts were recruited to the growth plate following the rapid differentiation and apoptosis of chondrocytes. *Ihh* and *PTH/PTHrP-R* mRNA, normally present in proliferating, transiting, and prehypertrophic chondrocytes (Lai and Mitchell, 2005), were also lost from the growth plate of mice after four doses of HhAntag, whereas the osteogenic marker genes (*MMP13*, *OPN*, and *BGP*) remained unchanged (Figure S7). These findings suggest that the majority of prehypertrophic and hypertrophic chondrocytes differentiated and died as a result of the transient blockade in Hh activity

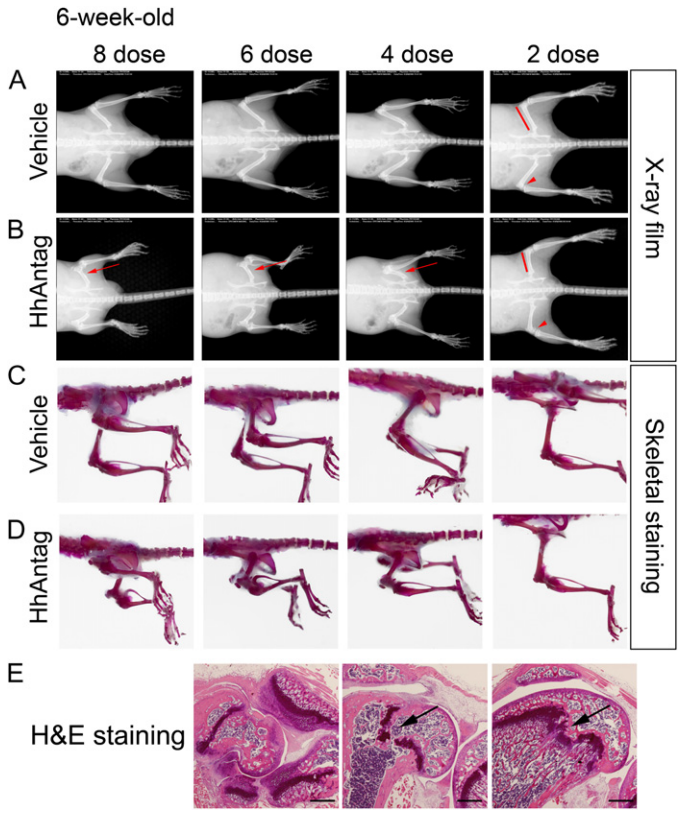

Figure 4. Severity of Bone Defects Correspond with Period of HhAntag Treatment

(A and B) Wild-type mice were treated with Vehicle (A) or 100 mg/kg HhAntag (B) twice daily by oral dosing from P10 to P11 (two dose), P10 to P12 (four dose), P10 to P13 (six dose) or P10 to P14 (eight dose). Red arrows and arrowheads indicate the femurs and knee joints, respectively. Soft X-ray images were taken when the mice reached 6 weeks of age.

(C and D) Skeletal structure stained with Alizarin Red S in whole mounts from 6-week-old mice treated with Vehicle (C) and HhAntag (D).

(E) H&E staining of cross sections of the femur in 6-week-old mice after HhAntag treatment. Scale bars indicate 500 μm.

leading to primary spongiosa formation. Microscopic analysis of H&E-stained sections of the growth plate from P16 mice, compared to those obtained from mice 2 days after treatment with HhAntag over the P10–P14 period, revealed dramatically enhanced bone remodeling (Figures 7A, 7B, 7E, and 7F). It seems that HhAntag initiated a series of biological processes that resulted in a massive expansion of the region involved in bone remodeling. Two days after treatment with HhAntag, the cartilage plate was drastically reduced, large spicules appeared (Figures 7A, 7B, 7E, and 7F), and osteoclasts and osteoblasts had invaded the growth plate, including the remaining hypertrophic zone (Figures 7C, 7D, 7G, and 7H). This process was not as well organized as the orderly synthesis of bone tissue occurring in normal bone (Figures 7A and 7E). Nevertheless, osteoblasts and osteoclasts actively remodeled the matrix and triggered trabecular bone formation (Figures 7F and 7H), followed by angiogenesis and incursion of bone marrow. Although the tissue organization is aberrant, it appears that the same cell types and bone remodeling processes, observed during normal bone development, are responsible for remodeling HhAntag-treated bones. However, the normal columnar organization normally associated with this process is lost, so the resulting bone structure is dysplastic.

HhAntag Removal Enhances Bone Mineral Deposition

ACF is characterized by the presence of cone-shaped epiphyses, premature fusion of the growth plate, and shortened stature (Hellemans et al., 2003). Here, we show that HhAntag-treated mice bear a striking resemblance to ACF. Therefore, we used micro-CT scanning to determine whether premature fusion of the femur growth plate also occurs in HhAntag-treated mice. Immediately following an eight dose treatment period, there were no obvious differences in the cartilage structure located between the epiphysis and diaphysis between control and treated mice (Figures 6F and 6G, Movies S1 and S2). However, the cortical bone adjacent to the primary spongiosa was clearly thinner after HhAntag treatment (Figure 8B). There was also reduced secondary ossification, in the spongy structure of existing bone (Figure 8B). In contrast, 2 days after removal of HhAntag, there was a dramatic increase in deposition of minerals in the growth plate and elimination of cartilage between the epiphysis and diaphysis (Figures 8A and 8B, Movies S3 and S4). Micro-CT data, captured at the location of endochondral ossification with exclusion of cortical bone (see Figure S8D), were used to calculate bone mineral densities (BMD) in treated and untreated mice (Figure 8C). Although no significant changes were observed during the course of HhAntag treatment, 2 days after removal of drug there was a 2-fold increase ($p = 0.0057$) in BMD in the growth plate. This suggests that during HhAntag treatment, expansion of the hypertrophic zone was not sufficient in itself to promote mineral deposition; however, removal of HhAntag was associated with a dramatic increase in bone mineralization. These findings demonstrate that transient exposure of young mice to HhAntag causes premature fusion of the growth plate and results in permanent defects in bone formation.

DISCUSSION

Transient Hh Pathway Inhibition Causes Permanent Bone Defects

We developed a vital imaging system for Hh pathway activity based on GliLuc transgenic mice. Using these mice, we demonstrated transient inhibition of Hh pathway activity following oral delivery of a small molecule antagonist of Smo (HhAntag). Remarkably, temporary inhibition of Smo activity in young mice induced a similar phenotype to that caused by conditional mutation of *Ihh* in postnatal chondrocytes (Maeda et al., 2007). In both cases, loss of Hh pathway activity rapidly resulted in differentiation of chondrocytes, expansion of the hypertrophic zone, and a breakdown in columnar organization. Restoration of Smo activity after drug removal precipitated bone mineralization and premature fusion of the growth plate. Although chondrocyte proliferation recovered, the population was significantly reduced. Disruption of growth plate structure led to shortened bones and aberrations of the articular surfaces that resulted in

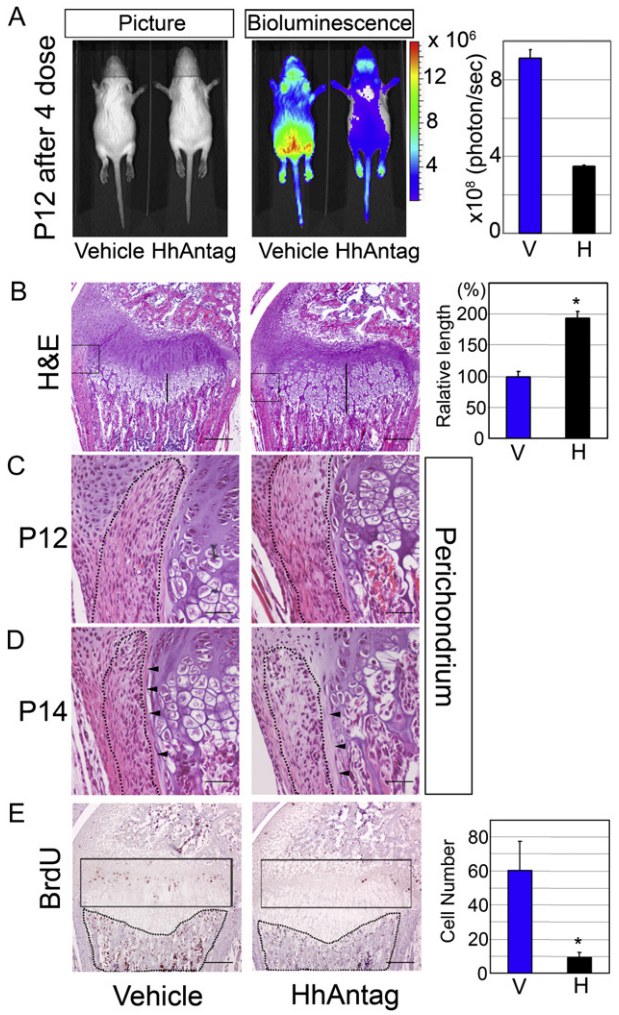

Figure 5. HhAntag Promotes Differentiation and Inhibits Proliferation of Chondrocytes

(A) Photograph, bioluminescence images, and quantitation of Hh pathway activity in P12 GliLuc transgenic mice after 2 days of treatment with Vehicle or 100 mg/kg HhAntag. Data indicate mean ± SD (n = 3).

(B) H&E staining of longitudinal cross-sections from the femurs of treated mice. Vertical lines indicate the extent of the prehypertrophic and hypertrophic chondrocytic layers. Graph illustrates the relative length of these layers measured from cross-sections (n = 6). Data indicate mean ± SD. Scale bars indicate 250 μm.

(C) Magnified view of the area indicated by black boxes in (B) showing the perichondrium at P12. Scale bar indicates 50 μm.

(D) View of the perichondium and surrounding tissue at P14 (magnified from Figure S5A). A dotted line outlines the perichondrium. Scale bar indicates 50 μm.

(E) BrdU labeling and immunostaining of longitudinal cross-sections from P14 femurs from Vehicle- and HhAntag-treated mice. The black box encloses chondrocytes in the proliferative zone. The region surrounded by a dotted line is primary spongiosa. The number of BrdU-positive cells in sections was counted (n = 6).

Values shown in graphs are mean ± SD. V, Vehicle; H, HhAntag. Scale bars indicate 250 μm. Asterisk indicates statistical significance by Student's t test with $p < 0.01$.

permanent defects in joint structures. These findings demonstrate that continuous Smo activity is required to maintain postnatal bone structures and that even transient loss of Hh signaling can result in long-term defects. Bone remodeling was not sufficient to overcome the structural alterations triggered by as little as 2 days of inhibition of Hh pathway activity in young mice. This result shows that short-term exposure to signal transduction inhibitors during development can have long-term consequences. Therefore, our findings raise concerns about the potential side effects associated with cancer therapies targeting the Hh pathway in children.

HhAntag Affects Developing Bone

During development, endochondral ossification relies on the maintenance of a strict zonal organization in the epiphyseal growth plate. The pathogenesis associated with HhAntag treatment is the consequence of a breakdown of this elegant structure. After a few days of HhAntag treatment, there is depletion of the proliferative zone, expansion of the zone of hypertrophy, and disruption of the columnar organization that underlies endochondral ossification. Removal of the drug reactivates the Hh pathway and promotes calcification and aberrant synthesis of trabecular bone. The formation of inappropriate bony trabeculae creates permanent structural alterations that cannot be removed by bone remodeling. Reduced proliferation and increased differentiation of condrocytes leads to shortening of the bones and dwarfism. These findings demonstrate the continuous need for Hh signaling in maintaining postnatal bone structures. Permanent deletion of *Ihh* in chondrocytes of mice carrying conditional and inducible null alleles of *Ihh* results in a similar phenotype to that reported here (Maeda et al., 2007; Razzaque et al., 2005), so clearly the pathway has an ongoing role in bone development. However, the remarkable finding reported here is that even temporary inhibition of Smo activity for as little as 48 hr is sufficient to disrupt bone development in young mice.

Previously, we treated adult mice for prolonged periods with HhAntag and observed no weight loss. In GliLuc mice, although the overall luciferase signal was much reduced in adults, there was a low but detectable signal level in skin (Figure 1D). However, this signal could not be inhibited by treatment with HhAntag (Figure S9), and therefore, it might be a consequence of basal Gli transcriptional activity that is not regulated by Smo. Several adult stem cell populations utilize Hh signaling (Ahn and Joyner, 2005; Mimeault and Batra, 2006), and they have the potential to be adversely affected by transient inhibition of the pathway. However, we have not observed any other deleterious effects of HhAntag treatment of adult mice, with the exception of a temporary inhibition of the continuous growth of incisor teeth (J. Romer and T.C., unpublished data), which is characteristic of adult mice but does not occur in humans. Thus, the effects observed here in young mice appear to be specific for developing bone and would not be expected to occur in healthy adults.

Inhibition of Bone Growth Requires Less HhAntag Than Antitumor Effects

Elimination of MB in $Ptc1^{+/-}p53^{-/-}$ mice requires 100 mg/kg HhAntag delivered orally twice a day for a period of 2 weeks (Romer et al., 2004; Sasai et al., 2006). At 20 mg/kg, there was still substantial residual tumor volume at the end of the 2 week period of treatment (Romer et al., 2004). When the drug was given for a shorter treatment period (4 days), there was little reduction in tumor volume, although there was a clear histological response

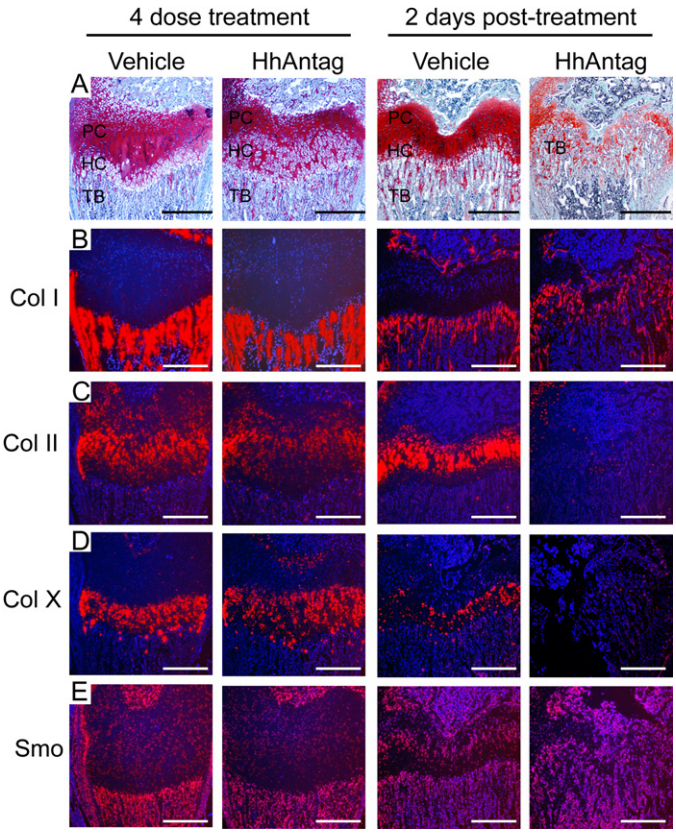

Figure 6. HhAntag Alters the Osteoblast and Chondrocyte Populations in the Growth Plate

(A–E) Safranin O staining (A) and in situ hybridization analysis (B–E) of bone markers in the femur growth plate of mice during and after treatment with 100 mg/kg HhAntag. P12 mice were analyzed after treatment for 2 days (four-dose treatment) or P16 mice after 4 days of treatment (eight dose) followed by a 2 day rest period. The probes used were *Col I* (B), *Col II* (C), *Col X* (D), and *Smo* (control, [E]). Images of RNA expression were visualized as red pseudocolor. PC, proliferative chondrocyte zone; HC, hypertrophic chondrocyte zone; TB, trabecular bone. Scale bars indicate 250 μm. Asterisk indicates statistically significant with Student's t test ($p < 0.01$).

and a dramatic drop in tumor cell proliferation. These results indicated that a prolonged period of exposure to high drug concentrations is required to eliminate tumor mass.

Pharmacokinetic studies indicated that HhAntag is rapidly cleared from the system so the levels of drug drop below the therapeutic threshold unless the dose is high (Romer et al., 2004). In contrast, the on-target side effect reported here requires only brief exposure to inhibitory concentrations of drug. We found that even as little as 10 mg/kg HhAntag substantially suppressed Hh pathway activity in skin after 2 days of treatment, and the effect was maximal at 25 mg/kg. Four days of treatment with 25 mg/kg HhAntag resulted in clear histological defects in bone structure. Suppressing the pathway with 100 mg/kg given twice daily caused permanent defects in bone structure after only 2 days of exposure. Thus, chondrocyte progenitor cells are highly susceptible to the effects of HhAntag. Previously, we found that HhAntag rapidly inhibits tumor cell proliferation but only modestly increases the rate of cell death. Therefore, the pathway may need to be completely suppressed in tumor cells for a prolonged period for tumor elimination. In contrast, even brief exposure of proliferating chondrocytes to HhAntag results in terminal differentiation. In an attempt to define a therapeutic window for HhAntag use in young mice, we treated five $Ptc1^{+/-}p53^{-/-}$ mice with 5 mg/kg HhAntag orally twice daily for 2 weeks starting on P10. Four of these mice developed medulloblastoma within 61 days (all controls developed medulloblastoma within 58 days), and one mouse survived to day 81, when the experiment was terminated. None of the treated mice showed any evidence of bone defects (Figure S10). These findings imply that it will not be possible to find a level of HhAntag that inhibits tumor growth in young mice without also causing defects in bone development.

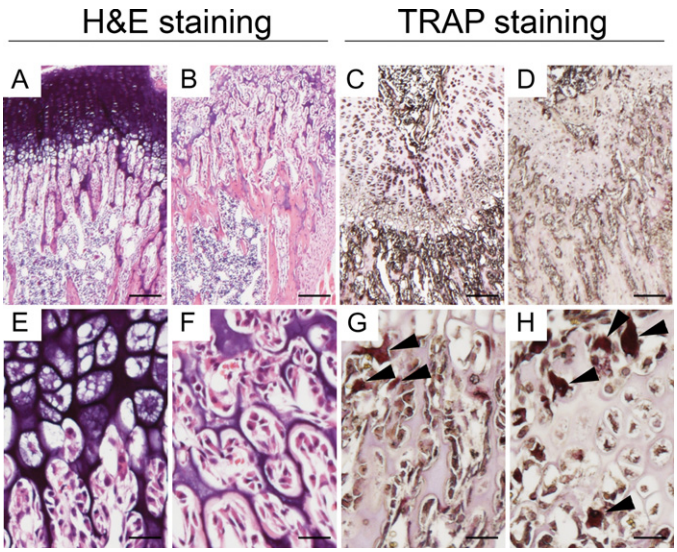

Figure 7. Osteoclasts Invade in the Expanded Primary Spongiosa Region after HhAntag Removal

(A, B, E, and F) H&E staining and (C, D, G, and H) TRAP staining in the growth plate of P16 mice after 4 days of treatment with (B, F, D, and H) or without (A, E, C, and G) 100 mg/kg HhAntag followed by a 2 day rest period. Arrowheads indicate TRAP-positive osteoclasts. Scale bars indicate 100 μm and 25 μm (E–H).

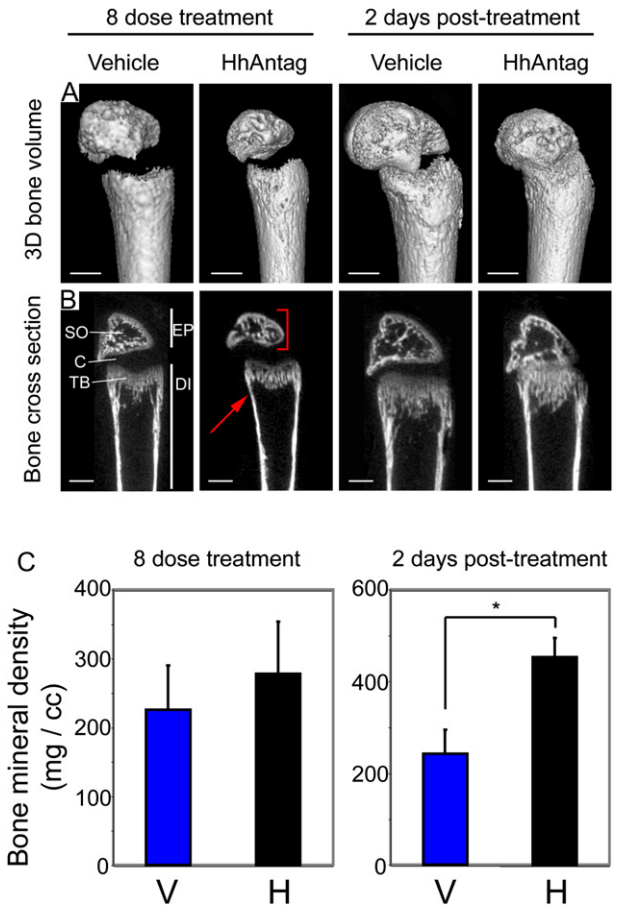

Figure 8. HhAntag Causes Premature Fusion of the Growth Plate and Increased Bone Mineral Density

(A and B) Micro-CT analyses of femurs from 14-day-old mice after 2 days of treatment (four dose) and 16-day-old mice after 4 days of treatment (eight dose) followed by a 2 day rest period. Scale bars indicate 500 μm. (A) Three-dimensional structural rendering of the femur. (B) Longitudinal cross-section CT images of the femur. EP, epiphysis; DI, diaphysis; SO, secondary ossification; C, cartilage; TB, trabecular bone. Red bracket and arrow indicate epiphysis and cortical bone abutting the perichondrium, respectively.

(C) Bone mineral density of trabecular bones in 20 slices from the front of endochondral ossification. V, Vehicle; H, HhAntag. Values shown at graphs are mean ± SD (eight-dose treatment, n = 4; 2 days posttreatment, n = 3). Asterisk indicates statistically significant by Student's t test with $p < 0.01$.

Hh Pathway Is a Target in Many Cancers

Several studies have suggested that the Hh pathway is a suitable target for therapeutic intervention in many cancers, not just those such as BCC and MB, that harbor Ptc1 mutations (Berman et al., 2003; Karhadkar et al., 2004; Sanchez et al., 2004; Watkins et al., 2003). In some cases, it has been suggested that upregulation of Hh ligands in tumors or stromal cells drives tumor cell proliferation, but in others the Hh pathway is thought to be important for maintenance of stromal cells and the cancer stem cell niche (Rubin and de Sauvage, 2006). Thus, the potential therapeutic indication of Hh pathway antagonists is quite broad. One note of caution, however, is that many of these studies employed cyclopamine in preclinical models to reach these conclusions. We found that the Hh pathway is rapidly downregulated in cultured medulloblastoma cells, and it does not recover when these cells are propagated in allografts (Sasai et al., 2006). Therefore, one should be cautious in interpreting the results of drug studies concerning inhibition of the Hh pathway based only on cell lines or tumors derived from cell lines. Furthermore, functional imaging of the Hh pathway in GliLuc mice allowed us to compare the efficacy of cyclopamine to that of HhAntag. We found that cyclopamine was less efficient at suppressing Hh pathway activity both in vitro and in vivo (Romer et al., 2004) (Figure S1). In addition, cyclopamine caused several serious side effects in young mice, including weight loss and dehydration, so we were not able to achieve a therapeutic dose in this model system. There are several possible explanations for the discrepancies with published studies. Each mouse strain may have differential sensitivity to cyclopamine, and it is also possible that young mice are more affected by the toxic side effects. In our experiments, we delivered cyclopamine by oral gavage, whereas other studies injected the compound so there may be differences in bioavailability using these different approaches. Nevertheless, it is difficult to interpret the effects of cyclopamine in vitro and in mouse models because of these issues.

Implications for Treatment of Human MB

Pediatric MB is the most common malignant primary central nervous system tumor of childhood with peak incidence at 7 years of age. Current therapy, involving a combination of surgery, radiation, and chemotherapy, is relatively successful with a 5 year survival rate of 78%. However, the prognosis is much worse for patients younger than 3 and in older patients with metastatic disease (Gilbertson, 2004). There is also significant morbidity associated with treatment, including endocrine and neuropsychological deficits, particularly in younger patients. Thus, there is a great need for alternative therapies.

At present, it is not clear that the developmental bone toxicities observed in mice would also occur in humans. Mice undergo extremely rapid bone growth during the period of treatment from P10 to P14. The period of most rapid bone growth in humans is just prior to the onset of puberty. It is possible that the exact age and duration of therapy could be chosen to minimize the impact on bone development. At present, it is difficult to gauge the extent of side effects that could be encountered in children to determine the cost versus the benefit of this therapeutic approach. Previously, we did not observe any major side effects after HhAntag treatment of adult mice (Romer et al., 2004). However, we must consider the possibility that transient inhibition of Hh pathway activity could result in compromised regenerative capacity in some adult tissues. These deficits may not be apparent until exposure of treated individuals to some form of physiological stress (e.g., surgery). Intramembranous ossification, although different from endochondral bone development, is affected by mutation of *Ihh*, and it is at least conceivable that cranium healing after surgery could be compromised.

To limit the potential side effects of Hh pathway inhibitors in pediatric brain tumor patients it is possible that drug targeting strategies may be adopted to limit the distribution of compounds to the craniospinal axis. In addition, while all of the blockers described to date appear to bind to the same target site on Smo, different chemical classes may distribute differentially, and it might be possible to identify compounds that selectively target

neuronal tissue. One can also consider strategies to protect bone tissue during the period of treatment. Thus, although the impact of a brief suppression of Hh pathway on bone development in mice is quite striking, this should not preclude attempts to develop a highly promising anticancer treatment for pediatric MB. MB also occurs, albeit at a lower incidence, in adults and in older children who have completed the majority of their growth. These patients, as well as adult or pediatric patients with recurrent disease, may well benefit from treatment with compounds specific for the Hh pathway. Hh pathway inhibitors could also be used at low doses in patients with germline mutations of *PTCH1* as cancer prevention agents or to reduce the other phenotypic consequences of increased pathway activity.

EXPERIMENTAL PROCEDURES

Generation of GliLuc Transgenic Mice

Six transgenic founder mice were identified following pronuclear injection of a transgene containing eight Gli binding sites fused to the luciferase gene (GliLuc) (Sasaki et al., 1997) into fertilized FVB/NJ oocytes. Mouse lines were propagated by crossing with FVB/NJ wild-type mice. Luciferase activity was confirmed using mouse embryonic fibroblasts (MEFs) and cerebellar granule cell cultures derived from GliLuc transgenic mice. Cells from only one line exhibited a robust increase in luciferase activity following treatment with Hh (data not shown). Reporter-positive mice were identified by PCR using primers to the promoter region 5′- CCGGGAACAGATTCGCGATCGACC-3′ and the luciferase gene 5′- CAGTTGCTCTCCAGCGGTTCCATC-3′.

Mice were housed in an American Association of Laboratory Animal Care-accredited facility and maintained in accordance with NIH Guidelines for the Care and Use of Laboratory Animals. The Institutional Animal Care and Use Committee at St. Jude Children's Research Hospital approved all procedures for animal use.

Bioluminescence Imaging and Luciferase Assays

Mice were anesthetized with intranasal isoflurane, and imaging was initiated 5 hr after the last drug treatment. D-Luciferin (150 mg/kg) in PBS was injected intraperitoneally prior to imaging. Bioluminescence imaging with a CCD camera (IVIS200, Xenogen) was carried out 5 min after injection of D-Luciferin. A 10 s bioluminescent image was captured in a 19.5 cm field of view, using a binning factor of 8, 1 f/stop, and an open filter. Signal intensities from regions of interest were defined manually, and data were expressed as total photon flux (photon per sec per area). Images (n = 3) were taken when luciferase signals reached steady state by IVIS200 (Xenogen) monitoring.

MEFs were prepared from E13.5 GliLuc mice and cultured in DMEM with 10% fetal bovine serum according to standard procedures. Tertiary fibroblasts were plated and cultured for 2 days until confluent at which point either Shh alone or Shh plus HhAntag were added to culture media. Two days later, luminescence images were taken following addition of D-Luciferin (1.5 mg/ml). Alternatively, cells were harvested, and cell extracts were prepared for luminescence assays according to manufacturer's specifications (Promega). Assays were performed in triplicate.

In Situ Hybridization

For bone tissues, paraffin sections were dewaxed, hydrated, and treated with proteinase K (20 μg/ml). Sections were treated with triethanolamine/acetic anhydride and dehydrated. Prehybridization and hybridization were performed at 50°C for 1 hr and overnight, respectively, using ^{35}S-UTP labeled riboprobes for *Col I*, *Col II*, *Col X*, and *Smo*. Slides were washed in 50% formamide/2 × SSC and treated with RNase A. After dehydration, slides were dipped in emulsion and exposed for 1–4 weeks. Slides were counterstained with Hoechst 33258. Images were captured using NIS-Elements software (Nikon).

Chemicals

HhAntagonist (HhAntag) was obtained from Genentech, Inc. (South San Francisco, CA). HhAntag is available from Genentech under a material transfer agreement, available at http://www.gene.com/gene/about/collaborations/contracts.jsp. HhAntag details are included in US patent WO 2003011219, available from the web site http://l2.espacenet.com/espacenet/viewer?PN=WO03011219. HhAntag was prepared in DMSO for tissue culture and in 0.5% Methylcellulose/0.2% Tween 80 for oral dosing. Cyclopamine (Toronto Research Chemicals) was suspended in 10% EtOH/90% Labrafil (GATTEFOSSE) for oral dosing.

Soft X-Ray and Skeletal Staining

Bone X-ray images were taken under anesthesia by Specimen Radiography System (Faxitron X-Ray Corp). Skeletons were prepared according to a modified protocol based on that of McLeod (McLeod, 1980). Adult mice were sacrificed, skinned, eviscerated in PBS, and fixed in 95% EtOH. Subsequently, acetone was used to remove fat. Then, skeletons were stained with 0.015% Alcian Blue and 0.005% Alizarin Red. Samples were cleared in 2% KOH overnight before transferring sequentially through 20% glycerol solution in 1% KOH for 7 days, 20% glycerol in 20% EtOH, and 50% glycerol in 50% EtOH overnight, respectively. Skeletons were stored in 100% glycerol.

Histopathology of Bone Tissues

Mice were injected with BrdU (100 mg/kg) in PBS 1 hr before perfusion with 4% paraformaldehyde (PFA) in PBS at 5 hr after the last Vehicle or HhAntag treatment. Bone samples were postfixed in 10% buffered formalin or 4% PFA and decalcified in 14% EDTA for 2 weeks or Morse's solution for 1 to 2 days at 4°C (Shibata et al., 2000). Bone tissues were embedded in paraffin. Thin sections (5 μm) were stained with hematoxylin and eosin (H&E) according to standard protocols. BrdU immunostaining was carried out according to the manufacturer's protocol (Zymed). Safranin O staining was performed in Wegret's iron hematoxylin working solution (Sigma), 0.001% fast green (FCF), and 0.1% Safranin O solutions (Sigma). The TRAP method for identifying osteoclasts was performed according to manufacturer's instructions (Sigma).

Micro-CT

After cardiac perfusion with 4% PFA, rear legs were dissected and fixed in 4% PFA at 4°C for 2 days, rinsed with PBS, and placed in 70% EtOH at 4°C. Femurs were scanned using GE explore Locus SP Pre-Clinical Specimen micro-CT operated at 16 μm isotropic voxel resolution. Bone tissues were computed with GE Healthcare MicroView software for visualization and analysis of volumetric image data.

SUPPLEMENTAL DATA

The Supplemental Data include ten supplemental figures and four supplemental movies and can be found with this article online at http://www.cancercell.org/cgi/content/full/13/3/249/DC1/.

ACKNOWLEDGMENTS

We thank Dr. Leyi Li for transgene microinjections. We also thank Drs. Lee Rubin (Curis) and Fred de Sauvage (Genentech) for providing Shh and HhAntag. We are grateful to Drs. Gerard Karsenty (*Col I* and *Col II*), Bjorn Olsen (*ColX*), Zena Werb, and Toshihisa Komori for providing reagents, and to Dr. Christopher Calabrese for assistance with micro-CT imaging. We also thank Drs. Tae-Ju Park, Alex Judkins, and Mark Solloway for critical comments on the manuscript. This work was supported by grant CA096832 from the National Institutes of Health (NIH).

Received: July 30, 2007
Revised: November 20, 2007
Accepted: January 14, 2008
Published: March 10, 2008

REFERENCES

Ahn, S., and Joyner, A.L. (2005). In vivo analysis of quiescent adult neural stem cells responding to Sonic hedgehog. Nature *437*, 894–897.

Arora, A., and Scholar, E.M. (2005). Role of tyrosine kinase inhibitors in cancer therapy. J. Pharmacol. Exp. Ther. *315*, 971–979.

Athar, M., Li, C., Tang, X., Chi, S., Zhang, X., Kim, A.L., Tyring, S.K., Kopelovich, L., Hebert, J., Epstein, E.H., Jr., et al. (2004). Inhibition of smoothened signaling prevents ultraviolet B-induced basal cell carcinomas through regulation of Fas expression and apoptosis. Cancer Res. *64*, 7545–7552.

Berman, D.M., Karhadkar, S.S., Hallahan, A.R., Pritchard, J.I., Eberhart, C.G., Watkins, D.N., Chen, J.K., Cooper, M.K., Taipale, J., Olson, J.M., and Beachy, P.A. (2002). Medulloblastoma growth inhibition by hedgehog pathway blockade. Science *297*, 1559–1561.

Berman, D.M., Karhadkar, S.S., Maitra, A., Montes De Oca, R., Gerstenblith, M.R., Briggs, K., Parker, A.R., Shimada, Y., Eshleman, J.R., Watkins, D.N., and Beachy, P.A. (2003). Widespread requirement for Hedgehog ligand stimulation in growth of digestive tract tumours. Nature *425*, 846–851.

Binns, W., James, L.F., Shupe, J.L., and Everett, G. (1963). A Congenital Cyclopian-Type Malformation in Lambs Induced by Maternal Ingestion of a Range Plant, Veratrum Californicum. Am. J. Vet. Res. *24*, 1164–1175.

Binns, W., Shupe, J.L., Keeler, R.F., and James, L.F. (1965). Chronologic evaluation of teratogenicity in sheep fed Veratrum californicum. J. Am. Vet. Med. Assoc. *147*, 839–842.

Callahan, C.A., and Oro, A.E. (2001). Monstrous attempts at adnexogenesis: Regulating hair follicle progenitors through Sonic hedgehog signaling. Curr. Opin. Genet. Dev. *11*, 541–546.

Chen, J.K., Taipale, J., Cooper, M.K., and Beachy, P.A. (2002). Inhibition of Hedgehog signaling by direct binding of cyclopamine to Smoothened. Genes Dev. *16*, 2743–2748.

Colnot, C., de la Fuente, L., Huang, S., Hu, D., Lu, C., St-Jacques, B., and Helms, J.A. (2005). Indian hedgehog synchronizes skeletal angiogenesis and perichondrial maturation with cartilage development. Development *132*, 1057–1067.

Cooper, M.K., Porter, J.A., Young, K.E., and Beachy, P.A. (1998). Teratogen-mediated inhibition of target tissue response to Shh signaling. Science *280*, 1603–1607.

Dellovade, T., Romer, J.T., Curran, T., and Rubin, L.L. (2006). The hedgehog pathway and neurological disorders. Annu. Rev. Neurosci. *29*, 539–563.

Ehlen, H.W., Buelens, L.A., and Vortkamp, A. (2006). Hedgehog signaling in skeletal development. Birth Defects Res. C Embryo Today *78*, 267–279.

Evangelista, M., Tian, H., and de Sauvage, F.J. (2006). The hedgehog signaling pathway in cancer. Clin. Cancer Res. *12*, 5924–5928.

Fogarty, M.P., Kessler, J.D., and Wechsler-Reya, R.J. (2005). Morphing into cancer: The role of developmental signaling pathways in brain tumor formation. J. Neurobiol. *64*, 458–475.

Fuchs, E. (2007). Scratching the surface of skin development. Nature *445*, 834–842.

Gabay, L., Lowell, S., Rubin, L.L., and Anderson, D.J. (2003). Deregulation of dorsoventral patterning by FGF confers trilineage differentiation capacity on CNS stem cells in vitro. Neuron *40*, 485–499.

Gilbertson, R.J. (2004). Medulloblastoma: Signalling a change in treatment. Lancet Oncol. *5*, 209–218.

Goodrich, L.V., Milenkovic, L., Higgins, K.M., and Scott, M.P. (1997). Altered neural cell fates and medulloblastoma in mouse patched mutants. Science *277*, 1109–1113.

Gorlin, R.J. (1995). Nevoid basal cell carcinoma syndrome. Dermatol. Clin. *13*, 113–125.

Hellemans, J., Coucke, P.J., Giedion, A., De Paepe, A., Kramer, P., Beemer, F., and Mortier, G.R. (2003). Homozygous mutations in IHH cause acrocapitofemoral dysplasia, an autosomal recessive disorder with cone-shaped epiphyses in hands and hips. Am. J. Hum. Genet. *72*, 1040–1046.

Kamachi, Y., and Kondoh, H. (1993). Overlapping positive and negative regulatory elements determine lens-specific activity of the delta 1-crystallin enhancer. Mol. Cell. Biol. *13*, 5206–5215.

Karhadkar, S.S., Bova, G.S., Abdallah, N., Dhara, S., Gardner, D., Maitra, A., Isaacs, J.T., Berman, D.M., and Beachy, P.A. (2004). Hedgehog signalling in prostate regeneration, neoplasia and metastasis. Nature *431*, 707–712.

Keeler, R.F. (1972). Effect of natural teratogens in poisonous plants on fetal development in domestic animals. Adv. Exp. Med. Biol. *27*, 107–125.

Kimura, H., Stephen, D., Joyner, A., and Curran, T. (2005). Gli1 is important for medulloblastoma formation in Ptc1+/− mice. Oncogene *24*, 4026–4036.

Lai, L.P., and Mitchell, J. (2005). Indian hedgehog: Its roles and regulation in endochondral bone development. J. Cell. Biochem. *96*, 1163–1173.

Maeda, Y., Nakamura, E., Nguyen, M.T., Suva, L.J., Swain, F.L., Razzaque, M.S., Mackem, S., and Lanske, B. (2007). Indian Hedgehog produced by postnatal chondrocytes is essential for maintaining a growth plate and trabecular bone. Proc. Natl. Acad. Sci. USA *104*, 6382–6387.

McLeod, M.J. (1980). Differential staining of cartilage and bone in whole mouse fetuses by alcian blue and alizarin red S. Teratology *22*, 299–301.

McMahon, A.P., Ingham, P.W., and Tabin, C.J. (2003). Developmental roles and clinical significance of hedgehog signaling. Curr. Top. Dev. Biol. *53*, 1–114.

Mimeault, M., and Batra, S.K. (2006). Concise review: Recent advances on the significance of stem cells in tissue regeneration and cancer therapies. Stem Cells *24*, 2319–2345.

Razzaque, M.S., Soegiarto, D.W., Chang, D., Long, F., and Lanske, B. (2005). Conditional deletion of Indian hedgehog from collagen type 2alpha1-expressing cells results in abnormal endochondral bone formation. J. Pathol. *207*, 453–461.

Romer, J.T., Kimura, H., Magdaleno, S., Sasai, K., Fuller, C., Baines, H., Connelly, M., Stewart, C.F., Gould, S., Rubin, L.L., and Curran, T. (2004). Suppression of the Shh pathway using a small molecule inhibitor eliminates medulloblastoma in Ptc1(+/−)p53(−/−) mice. Cancer Cell *6*, 229–240.

Rubin, L.L., and de Sauvage, F.J. (2006). Targeting the Hedgehog pathway in cancer. Nat. Rev. Drug Discov. *5*, 1026–1033.

Sanchez, P., Clement, V., and Ruiz i Altaba, A. (2005). Therapeutic targeting of the Hedgehog-GLI pathway in prostate cancer. Cancer Res. *65*, 2990–2992.

Sanchez, P., Hernandez, A.M., Stecca, B., Kahler, A.J., DeGueme, A.M., Barrett, A., Beyna, M., Datta, M.W., Datta, S., and Ruiz i Altaba, A. (2004). Inhibition of prostate cancer proliferation by interference with SONIC HEDGEHOG-GLI1 signaling. Proc. Natl. Acad. Sci. USA *101*, 12561–12566.

Sanchez, P., and Ruiz i Altaba, A. (2005). In vivo inhibition of endogenous brain tumors through systemic interference of Hedgehog signaling in mice. Mech. Dev. *122*, 223–230.

Sasai, K., Romer, J.T., Lee, Y., Finkelstein, D., Fuller, C., McKinnon, P.J., and Curran, T. (2006). Shh pathway activity is down-regulated in cultured medulloblastoma cells: Implications for preclinical studies. Cancer Res. *66*, 4215–4222.

Sasai, K., Romer, J.T., Kimura, H., Eberhart, D.E., Rice, D.S., and Curran, T. (2007). Medulloblastomas derived from Cxcr6 mutant mice respond to treatment with a smoothened inhibitor. Cancer Res. *67*, 3871–3877.

Sasaki, H., Hui, C., Nakafuku, M., and Kondoh, H. (1997). A binding site for Gli proteins is essential for HNF-3beta floor plate enhancer activity in transgenics and can respond to Shh in vitro. Development *124*, 1313–1322.

Savage, D.G., and Antman, K.H. (2002). Imatinib mesylate–a new oral targeted therapy. N. Engl. J. Med. *346*, 683–693.

Shibata, Y., Fujita, S., Takahashi, H., Yamaguchi, A., and Koji, T. (2000). Assessment of decalcifying protocols for detection of specific RNA by non-radioactive in situ hybridization in calcified tissues. Histochem. Cell Biol. *113*, 153–159.

Silvestri, G.A., and Rivera, M.P. (2005). Targeted therapy for the treatment of advanced non-small cell lung cancer: A review of the epidermal growth factor receptor antagonists. Chest *128*, 3975–3984.

St-Jacques, B., Hammerschmidt, M., and McMahon, A.P. (1999). Indian hedgehog signaling regulates proliferation and differentiation of chondrocytes and is essential for bone formation. Genes Dev. *13*, 2072–2086.

Thompson, M.C., Fuller, C., Hogg, T.L., Dalton, J., Finkelstein, D., Lau, C.C., Chintagumpala, M., Adesina, A., Ashley, D.M., Kellie, S.J., et al. (2006).

Genomics identifies medulloblastoma subgroups that are enriched for specific genetic alterations. J. Clin. Oncol. *24*, 1924–1931.

Watkins, D.N., Berman, D.M., Burkholder, S.G., Wang, B., Beachy, P.A., and Baylin, S.B. (2003). Hedgehog signalling within airway epithelial progenitors and in small-cell lung cancer. Nature *422*, 313–317.

Wetmore, C., Eberhart, D.E., and Curran, T. (2000). The normal patched allele is expressed in medulloblastomas from mice with heterozygous germ-line mutation of patched. Cancer Res. *60*, 2239–2246.

Wetmore, C., Eberhart, D.E., and Curran, T. (2001). Loss of p53 but not ARF accelerates medulloblastoma in mice heterozygous for patched. Cancer Res. *61*, 513–516.

Williams, J.A., Guicherit, O.M., Zaharian, B.I., Xu, Y., Chai, L., Wichterle, H., Kon, C., Gatchalian, C., Porter, J.A., Rubin, L.L., and Wang, F.Y. (2003). Identification of a small molecule inhibitor of the hedgehog signaling pathway: Effects on basal cell carcinoma-like lesions. Proc. Natl. Acad. Sci. USA *100*, 4616–4621.